THE UNIVERSITY *of* EDINBURGH

Edinburgh Research Explorer

Succinate is an inflammatory signal that induces IL-1 beta through HIF-1 alpha

OPEN ACCESS

Succinate is a danger signal that induces IL-1β via HIF-1α

GM Tannahill[1], **AM Curtis**[1], **J Adamik**[2], **EM Palsson-McDermott**[1], **AF McGettrick**[1], **G Goel**[3], **C Frezza**[4,5], **NJ Bernard**[1], **B Kelly**[1], **NH Foley**[1], **L Zheng**[4], **A Gardet**[6], **Z Tong**[7], **SS Jany**[1], **SC Corr**[1], **M Haneklaus**[1], **BE Caffery**[8], **K Pierce**[6], **S Walmsley**[9], **FC Beasley**[10], **E Cummins**[11], **V Nizet**[10], **M Whyte**[9], **CT Taylor**[11], **H Lin**[7], **SL Masters**[12], **E Gottlieb**[4], **VP Kelly**[1], **C Clish**[6], **PE Auron**[2,*], **RJ Xavier**[3,6,*], and **LAJ O'Neill**[1]

[1]School of Biochemistry and Immunology, Trinity Biomedical Sciences Institute, Dublin 2

[2]Department of Biological Sciences, Duquesne University, Pittsburgh, PA, 15282

[3]Centre for Computational and Integrative Biology, Massachussets General Hospital, Richard B. Simches Research Center, MA 02114

[4]Apoptosis and Tumour Physiology Lab, The Beatson Institute for Cancer Research, Bearsden, Glasgow

[5]Medical Research Council Cancer Cell Unit Hutchinson/MRC Research Centre, Hills road, Cambridge, CB2OX2

[6]The Broad Institute of MIT and Harvard, 7 Cambridge Center, Cambridge, MA 02142

[7]Department of Chemistry and Chemical Biology, Cornell University, Ithaca, NY 14853

[8]Smirfit Institute of Genetics, Trinity College Dublin, Dublin 2

[9]Academic Unit of Respiratory Medicine, Department of Infection and Immunity, University of Sheffield, Sheffield

[10]V Nizet Lab, Division of Pediatrics, Centre for Neural Circuits and Behaviour, University of California, La Jolla, California, 858-926-9001

[11]Conway Institute, University College Dublin, Dublin 4

[12]Inflammation Division, Walter and Eliza Hall Institute, 1G Royal Parade, Parkville, Victoria, 3052

Abstract

Macrophages activated by the gram negative bacterial product lipopolysaccharide (LPS) switch their core metabolism from oxidative phosphorylation to glycolysis[1]. Inhibition of glycolysis with 2-deoxyglucose (2DG) suppressed LPS-induced Interleukin-1 beta (IL-1β) but not Tumour necrosis factor alpha (TNFα) in macrophages. A comprehensive metabolic map of LPS-activated

Corresponding author: Luke A O'Neill. laoneill@tcd.ie.
*These authors contributed equally to this work

macrophages revealed up-regulation of glycolytic and down-regulation of mitochondrial genes, which correlated directly with the expression profiles of altered metabolites. LPS strongly increased the TCA cycle intermediate succinate. Glutamine-dependent anerplerosis was the major source of succinate with the 'Gamma-Aminobutyric Acid (GABA)-shunt' pathway also playing a role. LPS-induced succinate stabilized Hypoxia-inducible factor 1α (HIF-1α), an effect inhibited by 2DG, with IL-1β as an important target. LPS also increases succinylation of several proteins. Succinate is therefore identified as a metabolite in innate immune signalling which leads to enhanced IL-1β production during inflammation.

Activation of Toll-like receptors (TLRs), notably TLR4, leads to a switch from oxidative phosphorylation to glycolysis in immune cells[1,2], similar to that occurring in tumours. In bone marrow-derived macrophages (BMDMs) 2DG specifically inhibits LPS- and *Bordetella pertussis*- (*B pertussis*) induced IL-1β transcription, but not TNFα (Fig. 1a & 1b) or Interleukin-6 (IL-6) (Supplementary Fig. 1 & 2). 2DG had no effect on invasion and growth of the bacteria in BMDMs (Supplementary Fig. 3). The inhibitory effect of 2DG on LPS-induced IL-1β was evident *in vivo*. Inhibition of TNFα *in vivo* was also evident, most likely due to an IL-1β-dependency on induction of TNFα (Fig. 1c). There was no effect on the induction of IL-6 *in vivo* (Supplementary Fig. 4).

Supplementary Fig. 5 lists LPS-regulated genes affected by 2DG, including IL-1β. Several Hypoxia-inducible factor-1α (HIF-1α) targets were up-regulated by LPS and down-regulated with 2DG, including ankyrin repeat domain 37 (ANKRD37), lysyl oxidase (LOX) and cyclic AMP-dependent transcription factor 3 (ATF3).

LPS-induced HIF-1α protein but not mRNA expression in BMDMs was inhibited by 2DG. (Fig. 2a and Supplementary Fig. 6). To examine a direct functional relationship between HIF-1α and IL-1β we found LPS-induced IL-1β protein expression was dramatically increased under hypoxia (Fig. 2b), TNFα was not affected and as previously shown[3], IL-6 expression was inhibited (Supplementary Fig. 7). The prolyl hydroxylase (PHD) inhibitor Dimethyloxallyl Glycine (DMOG), which stabilises HIF-1α protein also boosted LPS-induced IL-1β mRNA (Supplementary Fig. 8). Conversely, pretreating LPS-stimulated BMDMs with a cell-permeable alpha-ketoglutarate (αKG) derivative, which increases PHD activity, depleting HIF-1α, significantly reduced LPS-induced IL-1β mRNA (Fig. 2c). αKG inhibited expression of both LPS-induced HIF-1α and IL-1β protein in a dose-dependent manner (Fig. 2d). Induction of IL-1β was attenuated in HIF-1α-deficient macrophages (Fig. 2e).

Inspection of human (*IL1B*) and murine (*Il1b*) gene sequences revealed a conserved canonical HIF-1α binding site approximately 300 bp upstream of the transcription start site in the human gene, and at position −357 in the mouse gene[4,5]. ChIP-PCR analysis in LPS stimulated BMDMs showed HIF-1α bound near the −300 position of *Il1b* at 4, 12 and 24 h, which was inhibited by 2DG. (Fig. 2f) LPS-induced *Il1b* luciferase activity, which was blocked by 2DG, had substantially reduced activity when −357 in the *Il1b* (Fig. 2g) or −300 in *IL1B* (Supplementary Fig. 9) promoter was mutated. LPS-induced HIF-1α binding to the −300 position of the *Il1b* promoter by ChIP analysis was abolished by pretreatment with αKG (Fig. 2h). Therefore IL-1β is a direct target of HIF-1α supporting previous data[6,7]. The

inhibition of IL-1β but not TNFα induction by 2DG is therefore explained by the HIF-1α dependency in the IL-1β gene. HIF-1α deficiency also rescues mice from LPS-induced sepsis[7] but how HIF-1α protein is regulated by LPS is still unknown.

Multiple groups have shown stabilization of HIF-1α by reactive oxygen species (ROS) following LPS stimulation[8,9], which we confirmed (Supplementary Fig. 10). Also, HIF-1α is stabilized via the PLC/PKC pathway[9], however treatment of BMDMs with specific inhibitors to PLC/PKC had no effect on LPS-induced HIF-1α protein expression at 24 hours (Supplementary Fig. 11).

Since both 2DG and αKG could inhibit HIF-1α accumulation and consequently induction of IL-1β, we hypothesized that the reported change in metabolism induced by LPS must be required for this response. We therefore next examined the metabolic profile of LPS-stimulated BMDMs by flux analysis, a metabolomic screen and microarray analysis. Extracellular flux analysis revealed increased glucose utilsation by LPS stimulated BMDMs (Fig. 3a). This is due to increased glycolysis as measured by an increase in extracellular acidification rate (ECAR) accompanied by a decrease in oxygen consumption rate (OCR) following LPS stimulation (Fig. 3a and Supplementary Fig. 12), confirming LPS induces the "Warburg Effect" of aerobic glycolsis.

The metabolomic screen confirmed this switch in metabolism with 73 metabolites changing out of 208 analysed (Supplementary Fig. 13). Glycolytic intermediates accumulated in 24 hours LPS stimulation. Despite decreased mitochondrial respiration, the TCA cycle intermediates, fumarate, malate and succinate accumulated. Succinate continued to accumulate between 4 and 24 hours, and isocitrate was significantly depleted. Despite a minor increase in citrate at 24 hours there was significant accumulation of di- and tri-acylglycerols, indicating an increased rate of fatty acid synthesis. Pentose Phosphate Pathway intermediates increased, as did the downstream products of purine and pyrimidine metabolism, guanosine, hypoxanthine and inosine (Supplementary Fig 13). These substrates are necessary to meet the increased demand for energy and nucleic acid synthesis of these highly active cells.

Microarray analysis revealed the metabolomic changes correlated with the gene expression profiles of LPS-stimulated BMDMs. 31 metabolic enzyme/transporter-related genes were differentially expressed at 24 hours LPS treatment (Supplementary Fig 14). The glucose transporter, GLUT1, hexokinase 3 (HK3), 6-phosphofructo-2-kinase/fructose-2,6-biphosphatase 3 (PFKFB3), phosphoglucomutase-2 (PGM2) and enolase 2 (ENO2), were significantly up-regulated, confirming an increase in glycolysis. Lack of mitochondrial activity can be explained by decreased expression of malate dehydrogenase (MDH1) and isocitrate dehydrogenase (IDH2). In addition, increased levels of citrate and Fatty Acids suggested that activity was being diverted away from the TCA cycle for biosynthetic needs. The metabolic screen and flux analysis therefore revealed that whilst there was an overall decrease in TCA cycle activity and mitochondrial respiration at 24 hours LPS treatment, there was an accumulation of the key TCA cycle intermediate, succinate.

Further analysis by LC-MS revealed that LPS caused a 30-fold increase in succinate at 24 hours, which equates to an increase in basal succinate from 25ng to 1ug per 2×10^6 cells. Pre-treatment with 2DG reduced intracellular succinate, in a dose dependent manner (Fig. 3b).

Succinate can be transported from the mitochondria *via* the dicarboxylic acid transporter to the cytosol where in excess it impairs PHD activity (by product inhibition) leading to HIF-1α stabilization and activation. This phenomenon has been defined as 'pseudohypoxia'[10]. This effect is blocked by αKG the substrate for PHD that generates succinate as a by-product in HIF-1α hydroxylation[10,11]. We had observed that αKG inhibited stabilization of HIF-1α and induction of IL-1β (Fig. 2), indicating that the stabilization of HIF-1α by LPS was likely to be dependent on the rise on succinate. We tested this further and found that cell-permeable diethylsuccinate alone had no effect on expression of HIF-1α (Supplementary Fig. 15) or IL-1β (Fig. 3c), since LPS is required to induce HIF-1α mRNA (Supplementary Fig. 6). However, in combination with LPS, succinate profoundly augmented IL-1β mRNA expression (Fig. 3C). This supports previous work in which succinate boosted LPS-induced IL-1β in dendritic cells[12]. Succinate levels are regulated by succinate dehydrogenase (SDH). Butylmalonate, an SDH inhibitor increased LPS-induced IL-1β mRNA (Fig. 3d). Both diethylsuccinate and butylmalonate increased HIF-1α and IL-1β protein in LPS-treated BMDMs (Supplementary Fig. 15). Diethylsuccinate also increased mRNA of the LPS-induced HIF-1α target, PHD3 (EGLN3)[13] (Supplementary Fig. 16). The effect of diethylsuccinate on IL-1β was due to HIF-1α as LPS-stimulated BMDMs from HIF-1α-deficient mice had less IL-1β protein and mRNA relative to WT, and pretreatment with diethylsuccinate had no significant effect. IL-6 and TNFα were unaffected in HIF-1α-deficient macrophages (Supplementary Fig 17). Therefore LPS-induced succinate can act as a signal to increase IL-1β expression through HIF-1α.

Certain metabolic enzymes have been shown to undergo succinylation[14]. We observed an increase in succinylation of proteins in response to LPS, which was reduced by 2DG in a dose dependent manner (Fig. 3e). This was confirmed by a ^{32}P-NAD assay (Supplementary Fig. S18). LPS treatment resulted in a two-fold increase in protein succinylation, which was inhibited by 36% with 2DG treatment (data not shown). The expression of SIRT5 (a recently reported desuccinylase and demalonylase[14]) was inhibited by LPS, suggesting reduced desuccinylase activity (Supplementary Fig 19). BMDMs treated for 24 hours with LPS also had a significantly altered NAD/NADH ratio favouring NADH, thus providing little NAD+ substrate for SIRT5 activity (Supplementary Fig 20). This decrease in the NAD/NADH ratio also provides further evidence of enhanced glycolysis and lower respiration. The increase in protein succinylation could therefore be explained by an increase in succinate and a decrease in the expression and activity of the desuccinylase SIRT5.

The relative abundance of proteins in BMDM lysates enriched using a succinyl lysine antibody were detected using LC-MS. Fig. 3f represents the mean emPAI values (relative quantity) of proteins from unstimulated and LPS-stimulated samples, an enrichment of succinylated proteins being evident in the LPS-treated BMDMs. The increased succinylation of malate dehydrogenase (Supplementary Table 1) has previously been reported in animal tissue[14]. Other proteins identified include glyceraldehyde-3-phosphate dehydrogenase,

glutamate carrier 1, L-lactate dehydrogenase A chain and transaldolase. The consequence of succinylation of these proteins, a covalent modification activated by LPS not previously reported, is currently under investigation.

A dysfunctional TCA cycle in LPS-stimulated BMDMs pointed towards an alternate source of succinate. The microarray screen revealed significantly higher levels of glutamine transporter (SLC3A2) at 24 hours. Succinate can be derived from glutamine through anerplerosis via αKG. We confirmed LPS-induction of SLC3A2 mRNA (Fig, 4a). SLC3A2 mRNA expression has previously been shown to increase during intestinal inflammation and is regulated by Sp1 and NFκB[15]. Blocking the NFκB pathway with a specific MyD88 inhibitory peptide significantly reduced LPS-induced SLC3A2 mRNA expression (Supplementary Fig. 21). Knockdown of SLC3A2 by siRNA in human PBMCs (Supplementary Fig. 22) significantly reduced LPS-induced IL-1β expression (Fig. 4b), but had no effect on IL-6 or TNFα (Supplementary Fig. 22). This was also demonstrated in the RAW-264 macrophage cell line (Supplementary Fig. 23).

In addition to anerplerosis, succinate can also be derived from glutamine via the "GABA shunt" pathway. Gene expression analysis and metabolomics revealed LPS-induced GABA transporters (SLC6A13, SLC6A12) and increased GABA production (Supplementary Fig. 13). The increase in GABA was confirmed by additional LC-MS analysis (Fig. 4c).

Next we traced the metabolism of $^{13}C_5,^{15}N_2$ labeled glutamine and measured the increase in $^{13}C_4$-succinate abundance in BMDMs treated with LPS for 24 hours (Fig. 4d). This revealed a marked increase in succinate production from labeled glutamine. $18.4\pm 0.9\%$ (n=4; $\pm$SEM) of the total succinate pool in the LPS-treated BMDMs was labeled after 3 hours incubation, as revealed by the ratio of $^{13}C_4$-succinate (heavy labeled succinate) to the sum of all measured succinate isotopomers. This represents a 14 fold increase in succinate relative to non-LPS- treated BMDMs. Treatment of BMDMs with the specific, irreversible inhibitor of the key "GABA shunt" enzyme GABA transaminase, vigabatrin[16], reduced the percentage of labeled succinate to $16.0 \pm 0.6\%$ (n=4; $\pm$SEM; p=<0.05), representing a 9.4 fold elevation over the levels of succinate attained with vigabatrin alone. This represented a 33% decrease compared to the samples from BMDMs not treated with vigabatrin (Fig. 4e). The elevation in succinate in response to LPS derived from glutamine is therefore largely from anerplerosis via αKG although a proportion is derived from the "GABA shunt".

Pretreatment of BMDMs with vigabatrin significantly reduced LPS-induced HIF-1α and IL-1β protein (Fig. 4f) as well as PHD3 mRNA (Supplementary Fig. 24). The inhibitory effect was specific for IL-1β as vigabatrin inhibited IL-1β mRNA expression (Fig. 4g) but not TNFα protein levels or IL-6 mRNA (Supplementary Fig. 24). This was also evident *in vivo* as a prescription formulation of vigabatrin (Sabril) reduced LPS-induced IL-1β (Fig. 4h) but had no effect on IL-6 (Supplementary Fig. 25). Similar to 2DG, the inhibitory effect of vigabatrin on TNFα is probably due to downstream signaling of IL-1β (Supplementary Fig. 25). Similarly vigabatrin reduced IL-1β serum levels in response to salmonella infection (Fig. 4I). This was consistent with the greater bacterial loading in the spleens of vigabatrin treated mice (Supplementary Fig. 26). In a model of sepsis, vigabatrin also protected mice, presumably by blocking HIF-1α activation (p<0.001) (Fig. 4j).

Our study therefore reveals that chronic activation of macrophages with LPS causes an increase in intracellular succinate via glutamine-dependent anerplerosis and the "GABA-shunt" pathway. Succinate acts as an endogenous danger signal to stabilize HIF-1α, which in turn specifically regulates gene expression of IL-1β and other HIF-1α-dependent genes and also leads to protein succinylation (Fig. 4k). The role of the "GABA shunt" is also of substantial interest. Vigabatrin is used clinically to treat epilepsy, as it can increase GABA, which is an inhibitory neurotransmitter. However adverse effects include significant increased risk of infections[17], which could be due to limitation of the GABA shunt in macrophages.

Succinate therefore joins other signals derived from mitochondria including cytochrome C[18], and mitochondrial DNA[19] that play a role in signaling cell trauma. Succinate can be released to signal through GPR91, which synergises with TLRs[12]. High succinate concentrations have been detected in the plasma of patients with peritonitis[20], and in the urine and plasma of diabetic and metabolic disease rodent models[21,22]. In addition, patients harbouring mutations in SDH have increased HIF-1α activity[23,24] and circulating succinate[25]. Succinate activates HIF-1α in tumours[10,26], indicating an important similarity between inflammation and cancer. The inflammatory process may have a tumorigenic effect by increasing succinate. The identification of succinate as a danger signal may therefore be important for our understanding of innate immunity in both inflammatory diseases and cancer.

Methods Section

Reagents

LPS used in *in vitro* and *in vivo* studies was from E. coli, serotype EH100 (Alexis) and 055:B5 (Sigma-Aldrich) respectively. 2DG (D3179), diethyl succinate (112402), diethyl butylmalonate (112402), vigabatrin (S (+)-γ-vigabatrin, V113), Gö6983 (PKC inhibitor) and N-acetyl cysteine (NAC) were all purchased from Sigma, U73122 (PLC inhibitor) from Calbiochem, DMOG (71210) from Cayman Chemicals, αKG, was a kind gift from Elaine MacKenzie in the Beatson Institute for Cancer Research, Glasgow and Sabril was a kind gift from Linda Cleary at Movianto, Dublin. Antibodies used were, anti-succinyl lysine (PTM Biolab, PTM-401), anti-IL-1β (R&D, AF401-NA), and anti-HIF-1α (Novus, NB100-449).

Microarray Profiling

Quantification of RNA concentration and purity was measured using the NanoDrop spectrophotometer (Thermo Scientific). The quality of the mouse RNA was ascertained using the Agilent Bioanalyser 2100 using the NanoChip protocol. A total of 500ng RNA was amplified and labeled using the Illumina TotalPrep RNA Amplification kit (Ambion) as per the manufacturer's instructions. A total of 1.5μg of labelled cRNA was then prepared for hybridization to the Illumina Mouse WG-6 chip. The Illumina microarray was performed by Partners HealthCare Center for Personalized Genetic Medicine (PCPGM) Core (Boston, USA).

Cellular Respiration and Extracellular acidification

XF24 Extracellular Flux analyser (Seahorse Biosciences) was used to determine the bioenergetic profile of LPS stimulated BMDMs. BMDMs were plated at 200,000 cells/well in XF24 plates overnight before being stimulated for up to 24h with LPS. OCR and ECAR were assessed in glucose containing media (seahorse Biosciences). Results were normalized to cell number.

Measurement of metabolites by LC-MS

Profiling of metabolites and lipids: Polar metabolites were profiled in the positive ion MS mode using an LC system comprised of a 1200 Series pump (Agilent Technologies) and an HTS PAL autosampler (Leap Technologies) that was coupled to a 4000 QTRAP mass spectrometer (AB SCIEX). Methanol extraction was carried on BMDMs. Samples were prepared by drying 100μL of cell extract under nitrogen and resuspending the residue in 100μL of 10/67.4/22.4/0.2 v/v/v/v water/acetonitrile/methanol/formic acid containing stable isotope-labeled internal standards (valine-d8, Sigma-Aldrich and phenylalanine-d8, Cambridge Isotope Laboratories). The samples were centrifuged (10 min, 10,000rpm, 4°C), and the supernatants were injected directly onto a 150×2.1 mm Atlantis HILIC column (Waters Corp.). Lipids were profiled in the positive ion mode using an 1100 Series pump and autosampler (Agilent Technologies) coupled to a QSTAR-XL MS system (AB SCIEX). MultiQuant software (version 1.2; AB SCIEX) was used to process all raw LC-MS data and integrate chromatographic peaks. The processed data were manually reviewed for quality of integration and compared against known standards to confirm metabolite identities. Succinate and GABA measurements: After stimulations, BMDMs were lysed with a solution kept in dry ice/methanol (−80°C) composed of 50% methanol and 30% acetonitrile in water and quickly scraped. The insoluble material was immediately pelleted in a cooled centrifuge (0°C) and the supernatant was collected for subsequent LC-MS analysis. A ZIC-HILIC column (4.6 mm × 150 mm, guard column 2.1 mm × 20 mm, Merck) was used for LC separation using formic acid, water acetonitrile as component of the mobile phase.

^{32}P-NAD assay

BMDMs were lysed for 30 min at 4°C in ice-cold lysis buffer (50mM Tris-HCl pH8, 150mM NaCl, 2mM EDTA, 0.1% NP-40, 10% glycerol), spun at 12,000rpm for 10 min and the supernatant was collected for trypsin digestion. 300μg of protein from each sample was dissolved in 6M Guanidine-HCl, 50mM Tris-HCl (pH 8.0), 15mM DTT in a reaction volume of 450μL. 22.5μL of 1M iodoacetamide was added and the mixture was incubated at room temperature with gentle shaking for 1 h. 20μL of 1M DTT was added with gentle mixing for 1h. 10μg of trypsin (Promega Cat# V51111) was added in the final buffer system (50mM Tris pH 7.4, 1mM CaCl$_2$) to digest proteins for 16 h at 37°C. The reaction was quenched by adding 67.5μL 10% TFA and the digested peptides were desalted by Sep-Pack C18 cartridge 1cc/50mg (Waters Corporation) and lyophilized. To detect the protein succinylation level in macrophages ± LPS was used to hydrolyze succinyl peptides using ^{32}P-NAD. Reactions were performed in 10μL solutions with 1μCi 32P-NAD (ARC Inc., ARP 0141, 800Ci/mmol, 0.125μM), 50mM Tris-HCl (pH 8.0), 150mM NaCl, 1mM DTT. 100μM synthetic H3K9 succinyl and malonyl peptides were used as positive controls.

100μg macrophage trypsin digested peptides were used as substrates. The reactions were incubated with 4μM SIRT5 at 37°C for 2h. A total of 0.5μL of each reaction mixture were spotted onto silica gel TLC plates and developed with 7:3 ethanol: ammonium bicarbonate (1M aqueous solution). The plates were further air-dried and exposed by PhosphoImaging screen (GE Healthcare) overnight. The signal was detected using a STORM860 phosphorimager (GE Healthcare).

Identification of proteins by LC-MS/MS in a succinyl-lysine pull-down

LPS-treated BMDMs were lysed as above. Anti-succinyl lysine antibody, or non-specific Rabbit IgG in control sample, were pre-coupled to protein A/G agarose beads, washed, and incubated with the cell lysates for 2h at 4°C. The immune complexes were precipitated and washed thoroughly in lysis buffer. The protein was eluted by adding sample buffer and was subsequently separated by SDS–polyacrylamide gel electrophoresis (PAGE) and gel slices ranging from 35 – 40 kDa and 55 – 65 kDa were subjected to 1D nLC-MS/MS mass spectrometry using a LTQ Orbitrap Velos Pro. Peptides were identified with Mascot (Matrix Sciences) against the Mouse IPI database with a protein score cut-off of 37. The emPAI values of proteins of appropriate molecular weight, excluding non-specifically bound proteins with highest values in the IgG control sample as well as keratin and IP antibody contaminations, were used to estimate relative abundance in the samples. Enrichment of proteins was statistically analyzed using an unpaired, two-sided t-test for the mean emPAI values.

Endotoxin-induced model of sepsis

Mice were treated ± vigabatrin (400mg/kg) or PBS for 30 min. Sepsis was induced by injecting 60mg/kg of LPS and survival was monitored. Mice were culled immediately at a humane end-point.

Supplementary Material

Refer to Web version on PubMed Central for supplementary material.

Acknowledgments

References

1. Rodriguez-Prados JC, et al. Substrate fate in activated macrophages: a comparison between innate, classic, and alternative activation. J Immunol. 2010; 185:605–614.10.4049/jimmunol.0901698 [PubMed: 20498354]

2. Krawczyk CM, et al. Toll-like receptor-induced changes in glycolytic metabolism regulate dendritic cell activation. Blood. 2010; 115:4742–4749.10.1182/blood-2009-10-249540 [PubMed: 20351312]

3. Pan H, Wu X. Hypoxia attenuates inflammatory mediators production induced by Acanthamoeba via Toll-like receptor 4 signaling in human corneal epithelial cells. Biochem Biophys Res Commun. 2012; 420:685–691.10.1016/j.bbrc.2012.03.069 [PubMed: 22450324]

4. Hiscott J, et al. Characterization of a functional NF-kappa B site in the human interleukin 1 beta promoter: evidence for a positive autoregulatory loop. Mol Cell Biol. 1993; 13:6231–6240. [PubMed: 8413223]

5. Ghisletti S, et al. Parallel SUMOylation-dependent pathways mediate gene-and signal-specific transrepression by LXRs and PPARgamma. Mol Cell. 2007; 25:57–70.10.1016/j.molcel. 2006.11.022 [PubMed: 17218271]

6. Zhang W, et al. Evidence that hypoxia-inducible factor-1 (HIF-1) mediates transcriptional activation of interleukin-1beta (IL-1beta) in astrocyte cultures. J Neuroimmunol. 2006; 174:63–73.10.1016/j.jneuroim.2006.01.014 [PubMed: 16504308]

7. Peyssonnaux C, et al. Cutting edge: Essential role of hypoxia inducible factor-1alpha in development of lipopolysaccharide-induced sepsis. J Immunol. 2007; 178:7516–7519. [PubMed: 17548584]

8. Chandel NS, et al. Reactive oxygen species generated at mitochondrial complex III stabilize hypoxia-inducible factor-1alpha during hypoxia: a mechanism of O2 sensing. J Biol Chem. 2000; 275:25130–25138.10.1074/jbc.M001914200 [PubMed: 10833514]

9. Sumbayev VV. LPS-induced Toll-like receptor 4 signalling triggers cross-talk of apoptosis signal-regulating kinase 1 (ASK1) and HIF-1alpha protein. FEBS Lett. 2008; 582:319–326.10.1016/j.febslet.2007.12.024 [PubMed: 18155167]

10. Selak MA, et al. Succinate links TCA cycle dysfunction to oncogenesis by inhibiting HIF-alpha prolyl hydroxylase. Cancer Cell. 2005; 7:77–85.10.1016/j.ccr.2004.11.022 [PubMed: 15652751]

11. Koivunen P, et al. Inhibition of hypoxia-inducible factor (HIF) hydroxylases by citric acid cycle intermediates: possible links between cell metabolism and stabilization of HIF. J Biol Chem. 2007; 282:4524–4532.10.1074/jbc.M610415200 [PubMed: 17182618]

12. Rubic T, et al. Triggering the succinate receptor GPR91 on dendritic cells enhances immunity. Nat Immunol. 2008; 9:1261–1269.10.1038/ni.1657 [PubMed: 18820681]

13. Walmsley SR, et al. Prolyl hydroxylase 3 (PHD3) is essential for hypoxic regulation of neutrophilic inflammation in humans and mice. J Clin Invest. 2011; 121:1053–1063.10.1172/JCI43273 [PubMed: 21317538]

14. Du J, et al. Sirt5 is a NAD-dependent protein lysine demalonylase and desuccinylase. Science. 2011; 334:806–809.10.1126/science.1207861 [PubMed: 22076378]

15. Yan Y, Dalmasso G, Sitaraman S, Merlin D. Characterization of the human intestinal CD98 promoter and its regulation by interferon-gamma. Am J Physiol Gastrointest Liver Physiol. 2007; 292:G535–545.10.1152/ajpgi.00385.2006 [PubMed: 17023546]

16. Choi S, Silverman RB. Inactivation and inhibition of gamma-aminobutyric acid aminotransferase by conformationally restricted vigabatrin analogues. J Med Chem. 2002; 45:4531–4539. [PubMed: 12238932]

17. Walker SD, Kalviainen R. Non-vision adverse events with vigabatrin therapy. Acta Neurol Scand Suppl. 2011:72–82.10.1111/j.1600-0404.2011.01602.x [PubMed: 22061182]

18. Bossy-Wetzel E, Newmeyer DD, Green DR. Mitochondrial cytochrome c release in apoptosis occurs upstream of DEVD-specific caspase activation and independently of mitochondrial transmembrane depolarization. EMBO J. 1998; 17:37–49.10.1093/emboj/17.1.37 [PubMed: 9427739]

19. Zhang Q, et al. Circulating mitochondrial DAMPs cause inflammatory responses to injury. Nature. 2010; 464:104–107.10.1038/nature08780 [PubMed: 20203610]

20. Rotstein OD, Pruett TL, Simmons RL. Lethal microbial synergism in intra-abdominal infections. Escherichia coli and Bacteroides fragilis. Arch Surg. 1985; 120:146–151. [PubMed: 3156575]

21. Toma I, et al. Succinate receptor GPR91 provides a direct link between high glucose levels and renin release in murine and rabbit kidney. J Clin Invest. 2008; 118:2526–2534.10.1172/JCI33293 [PubMed: 18535668]

22. Sadagopan N, et al. Circulating succinate is elevated in rodent models of hypertension and metabolic disease. Am J Hypertens. 2007; 20:1209–1215.10.1016/j.amjhyper.2007.05.010 [PubMed: 17954369]

23. Gimenez-Roqueplo AP, et al. The R22X mutation of the SDHD gene in hereditary paraganglioma abolishes the enzymatic activity of complex II in the mitochondrial respiratory chain and activates

the hypoxia pathway. Am J Hum Genet. 2001; 69:1186–1197.10.1086/324413 [PubMed: 11605159]

24. Dahia PL, et al. A HIF1alpha regulatory loop links hypoxia and mitochondrial signals in pheochromocytomas. PLoS Genet. 2005; 1:72–80.10.1371/journal.pgen.0010008 [PubMed: 16103922]

25. Hobert JA, Mester JL, Moline J, Eng C. Elevated plasma succinate in PTEN, SDHB, and SDHD mutation-positive individuals. Genet Med. 2012; 14:616–619.10.1038/gim.2011.63 [PubMed: 22261759]

26. Pistollato F, et al. Hypoxia and succinate antagonize 2-deoxyglucose effects on glioblastoma. Biochem Pharmacol. 2010; 80:1517–1527.10.1016/j.bcp.2010.08.003 [PubMed: 20705058]

27. MacKenzie ED, et al. Cell-permeating alpha-ketoglutarate derivatives alleviate pseudohypoxia in succinate dehydrogenase-deficient cells. Mol Cell Biol. 2007; 27:3282–3289.10.1128/MCB. 01927-06 [PubMed: 17325041]

28. Masters SL, et al. Activation of the NLRP3 inflammasome by islet amyloid polypeptide provides a mechanism for enhanced IL-1beta in type 2 diabetes. Nat Immunol. 2010; 11:897–904.10.1038/ni. 1935 [PubMed: 20835230]

29. Doyle SL, et al. The GOLD domain-containing protein TMED7 inhibits TLR4 signalling from the endosome upon LPS stimulation. Nat Commun. 2012; 3:707.10.1038/ncomms1706 [PubMed: 22426228]

30. West AP, et al. TLR signalling augments macrophage bactericidal activity through mitochondrial ROS. Nature. 2011; 472:476–480.10.1038/nature09973 [PubMed: 21525932]
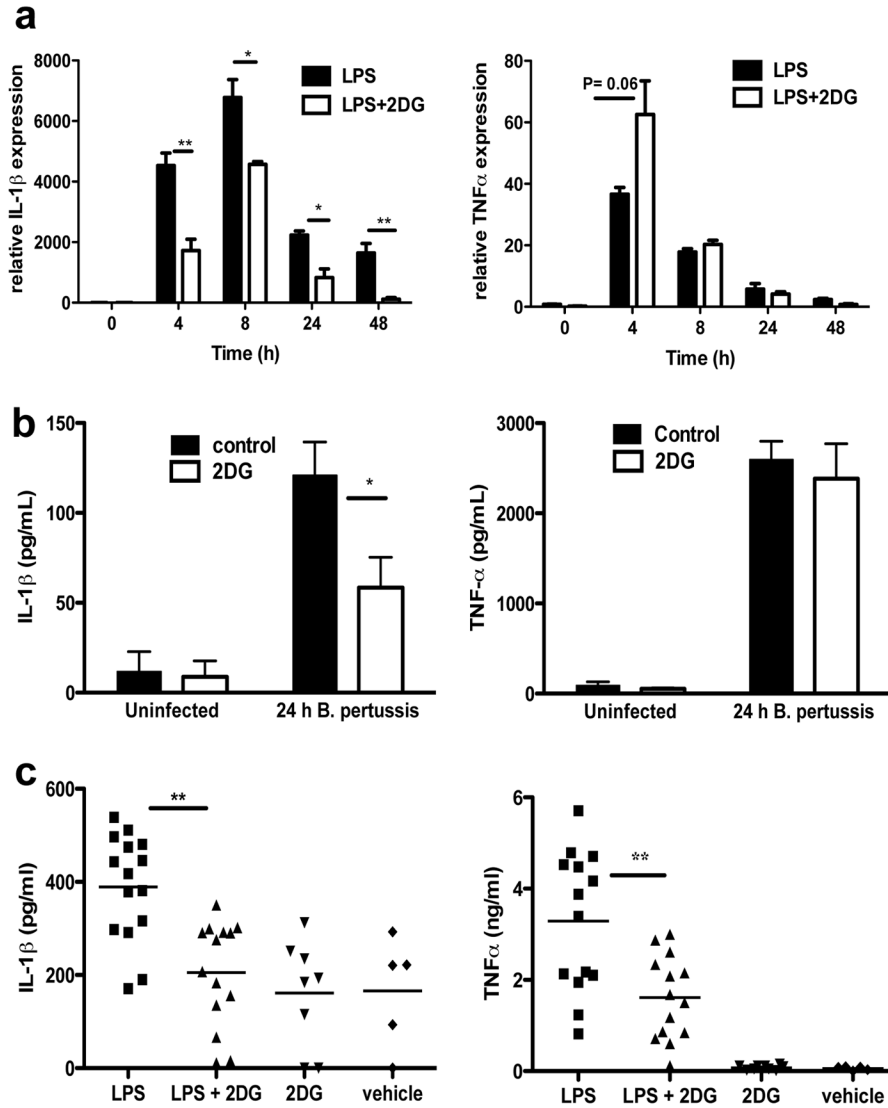
Fig. 1. Glycolysis is necessary for LPS-induced IL-1β expression
(A, B) IL-1β and TNFα mRNA in 100ng/ml LPS- or 1×10^5 *B pertussis*- stimulated BMDMs ± 2DG (1mM) pretreatment for 3h (n=3). (C) Mice i.p. injected ± 2DG (2g/kg) or PBS for 3h, then 15 mg/kg LPS or PBS for 1.5h. Serum levels of IL-1β and TNFα (LPS n=15; LPS+2DG n=14; 2DG n=8; vehicle n=5). Error bars, s.e.m, * p < 0.05; ** p < 0.01.
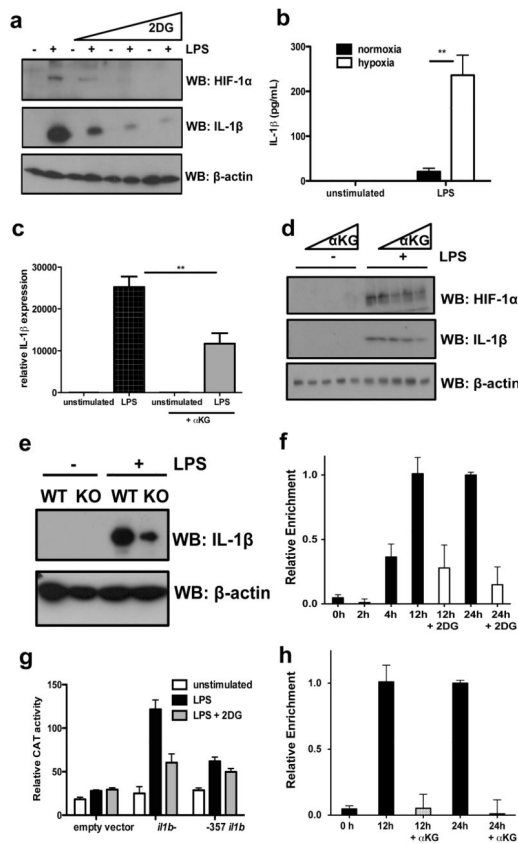
Fig. 2. HIF-1α is responsible for LPS-induced IL-1β expression

(A) LPS-induced HIF-1α and IL-1β protein expression ± 2DG (1, 5, 10mM). (B) IL-1β in BMDMs incubated in normoxia or hypoxia for 24h then LPS for 24h. (C) IL-1β mRNA in LPS-stimulated BMDMs pretreated ± αKG derivative[27] (1mM). (D) LPS-induced HIF-1β and IL-1β in BMDMs pretreated ± αKG (0.01, 1, 100, 1000μM). (E) LPS-induced IL-1β protein in WT and HIF-1α-deficient BMDMs. (F) ChIP-PCR using HIF-1α antibody and primers specific for −300 position of *il1b* in LPS-treated BMDMs ±2DG (1mM). (G) Reporter activity in RAW-264 cells transfected with il1b- or −357 il1b. Representative of 3 experiments. Error bars, s.d. (I) ChIP-PCR as above in BMDMs treated with LPS ±αKG (1mM). Error bars, s.e.m, ** p < 0.01.
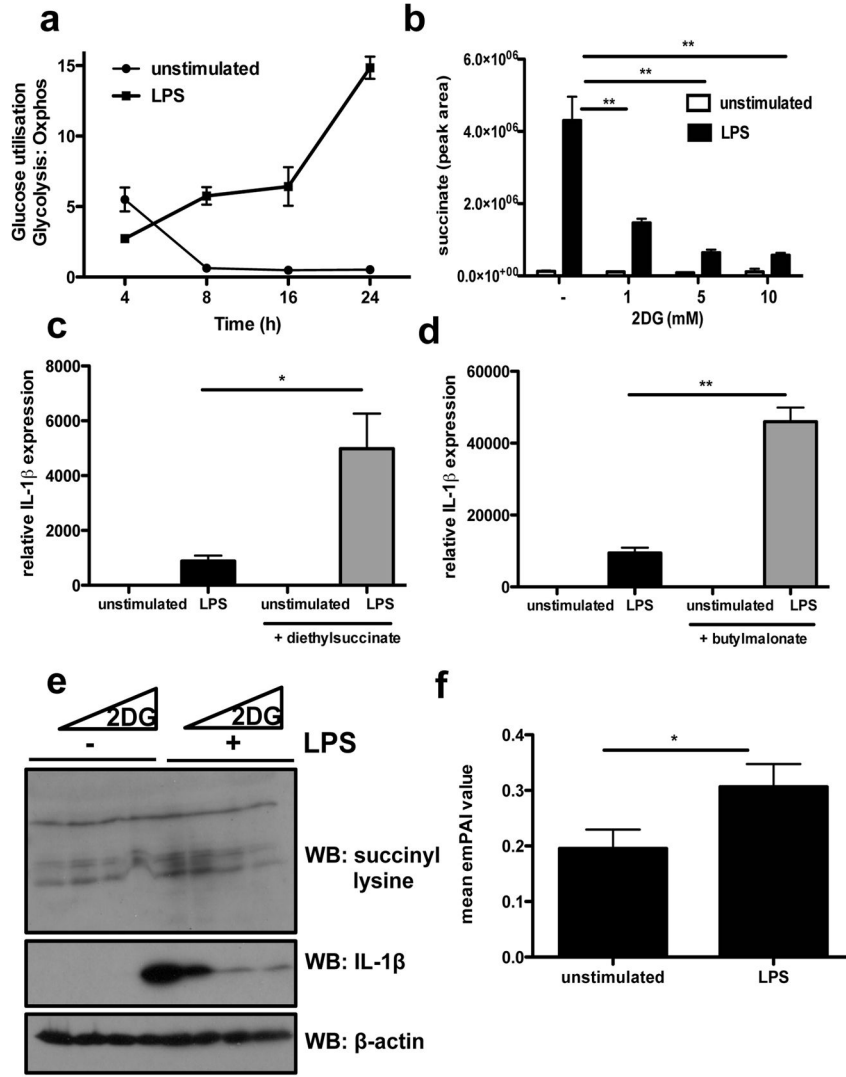
Fig. 3. Succinate is induced by LPS to drive HIF-1α-induced IL-1β expression
(A) Glucose utilization over time, as a ratio of ECAR:OCR in LPS-treated BMDMs, analysed on the Seahorse XF-24. (B) Succinate abundance in LPS-stimulated BMDMs pretreated ± 2DG (1, 5, 10mM). (C, D) LPS-stimulated BMDMs pretreated ± 5mM diethylsuccinate or butylmalonate (1mM) for 3 h. n=3. (E) Succinyl-lysine expression and corresponding IL-1β in LPS-stimulated BMDMs ± 2DG (1, 5, 10mM) pretreatment for 3h. (J) Average emPAI values (exponentially modified protein abundance index) as a measure of relative abundance of proteins listed in Supplementary Table 1. Error bars, s.e.m, * p < 0.05; ** p < 0.01.
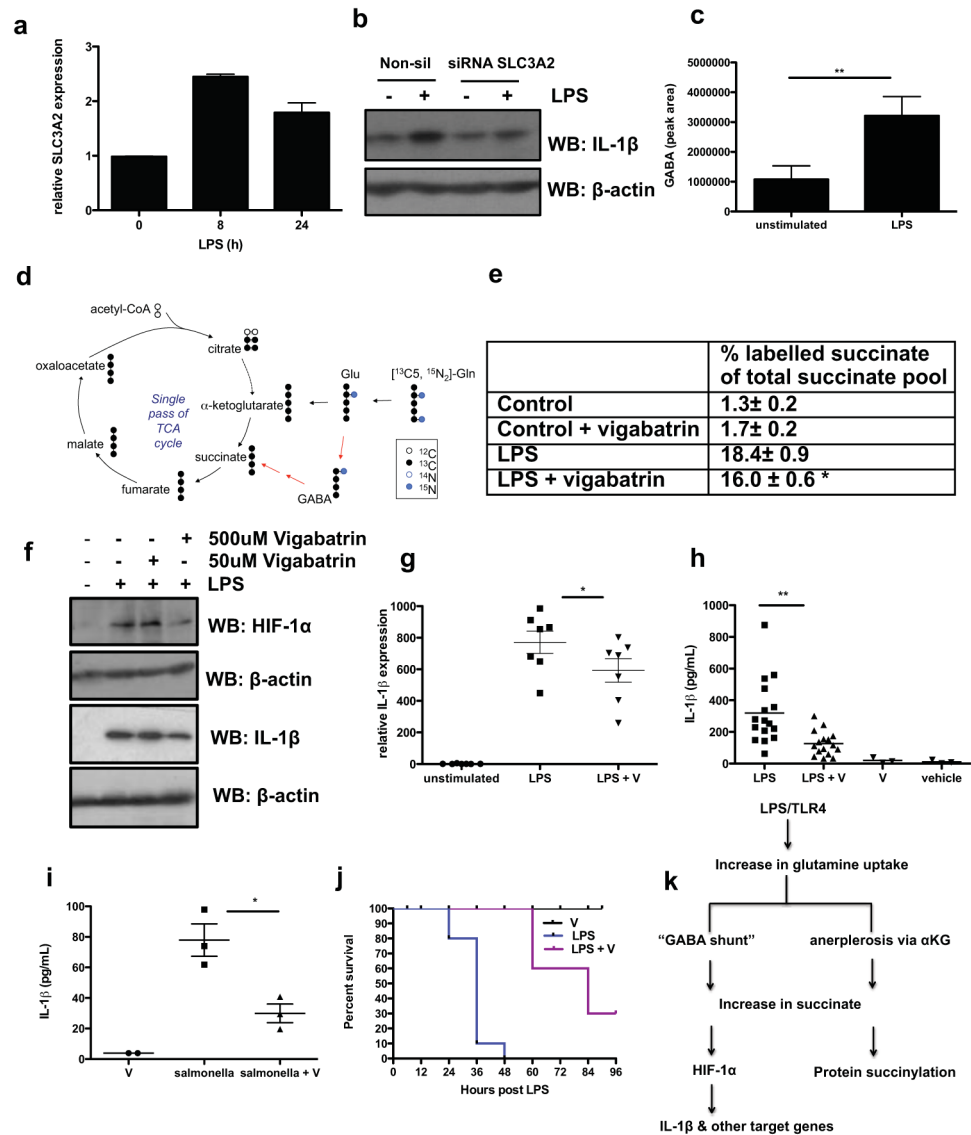
Fig. 4. Glutamine is the source of LPS-induced succinate

(A) SLC3A2 mRNA in LPS-treated BMDMs for 8 and 24h. (B) IL-1β in human PBMCs transfected with 100nM SLC3A2 siRNA compared non-silencing control. Representative of 3 experiments. (C) GABA abundance in serum-deprived BMDMs stimulated with 10ng/ml LPS for 24h. (D) Schematic representing tracing of $^{13}C_5, ^{15}N_2$ labelled glutamine in BMDMs treated with LPS for 24h. (E) LPS-stimulated BMDMs pretreated ± vigabatrin (500μM) for 20h then 1mM $^{13}C_5, ^{15}N_2$ glutamine for 4h. Table represents ratio of $^{13}C_4$-succinate to the sum of all measured succinate isotopomers as measured by LC-MS. The values shown are mean ± s.e.m, n=4. (F, G) LPS-induced HIF-1α and IL-1β protein and IL-1β mRNA (n=7) in BMDMs pretreated ± vigabatrin for 30 min. (H) IL-1β in serum from mice i.p. injected ± vigabatrin (400mg/kg) or PBS for 1.5h, then 15 mg/*kg* LPS or PBS solution for 1.5h (LPS n=16; LPS+vigabatrin (LPS + V) n=14; vigabatrin (V) n=3; vehicle n=3). (I) IL-1β in serum from mice i.p. injected ± vigabatrin (400mg/kg) or PBS for 1.5h

then infected with 1×10^6 *Salmonella* Typhimurium UK1 i.p. for 2h (J) Survival of mice i.p. injected ± vigabatrin (400mg/kg) or PBS for 1.5h, then 60 mg/kg LPS or PBS (PBS n=10 (not shown), vigabatrin n=10, LPS n=10, LPS + vigabatrin n=10). Error bars, s.e.m, * p < 0.05; ** p < 0.01. (K) Proposed model: LPS induces high levels of succinate to drive HIF-1α-dependent IL-1β expression and protein succinylation.